

The Mean-Field Ground-State Phase Diagram of the Half-Filled Mass-Imbalanced $t - t'$ Ionic-Hubbard Chain

Shota Garuchava* and George Japaridze**

*Faculty of Natural Sciences and Medicine, Ilia State University, Tbilisi, Georgia

**Academy Member, Andronikashvili Institute of Physics, Tbilisi, Georgia

We investigate the ground-state (GS) phase diagram of the one-dimensional tight-binding Hubbard model of spin 1/2 free fermions, with spin-dependent nearest-neighbor ($t_{\uparrow} \neq t_{\downarrow}$) and next-nearest-neighbor ($t'_{\uparrow} \neq t'_{\downarrow}$) hopping in the presence of a staggered ionic potential Δ , for various values of the mass-imbalance parameter $\eta = t'_{\uparrow} / t'_{\downarrow} = t_{\uparrow} / t_{\downarrow}$ ($0 < \eta < 1$), as a function of the frustration ratio $\zeta = t'_{\sigma} / t_{\sigma}$ and the Hubbard repulsion U . Phase diagram is constructed in the case of half-filled band and zero net magnetization, where the average density of particles per site $\langle \rho_{\uparrow} \rangle = \langle \rho_{\downarrow} \rangle = 1/2$. Connection between the peculiarities of the GS phase diagram of the interacting system and the topological Lifshitz transition, with increasing ζ , in the GS of free particle chain is discussed. The mean-field Hamiltonian is characterized by two order parameters, Δ_{\uparrow} and Δ_{\downarrow} , which are determined self-consistently. It is shown that the GS phase diagram consists of four distinct phases: band-insulator (BI), correlated-insulator (CI), metal and half-metal. In the latter, the system shows gapped insulating behavior for one spin component and gapless metallic – for the other. © 2023 Bull. Georg. Natl. Acad. Sci.

ultra cold atoms, optical lattices, spin-dependent hopping

The ability to control and manipulate electron spins with an efficiency comparable to that of present-day (charge) electronics is one of the major goals of modern spintronics [1]. Electrical current can be completely spin polarized in a class of materials known as half-metals, as a result of the coexistence of metallic nature for electrons with one spin orientation and insulating for electrons with the other [2]. Thus the study of electronic models opening the possibility for realization in the ground state of phases characterized by the presence of spin-selective metallic properties is of major importance.

Atomic gases stored in artificially engineered optical lattices constitute structures beyond those currently achievable in actual materials and, thanks to the easy manipulation of parameters, serve as a playground for the simulation of condensed-matter systems with unconventional properties [3]. Clean and precisely controlled environment of ultracold atoms in optical lattices allows a direct simulation of an

inaccessible in real materials physical reality onto such models. Moreover, the possibility of manipulating the interaction strength using the Feshbach resonance [4] enables the observation of many-body phenomena from weak to strong coupling. Optical lattices can be generated in various geometries, including bipartite lattices with different potential minima on the two sublattices [5]. Another advantage of the cold atoms trapped in optical lattices is the possibility to use two atom species with different masses [6], which has opened wide possibilities in experimental realization of low-dimensional correlated fermion models with spin-dependent hopping. Theoretical predictions of various unconventional superfluid or superconducting [7], insulating [8], and magnetic [9] phases in bosonic and fermionic Hubbard models with spin-dependent hopping have further stimulated the interest in studies of correlated fermion models with the spin-asymmetric hopping [10-15].

The Model

In this paper we consider the ground state phase diagram of the tight-binding fermions on a bipartite lattice (sub-lattices A and B) described by the following Hamiltonian

$$H = \sum_{n,\sigma} (-t_\sigma c_{n,\sigma}^\dagger c_{n+1,\sigma} + t'_\sigma c_{n,\sigma}^\dagger c_{n+2,\sigma} + \text{H.c.}) + \frac{\Delta}{2} \sum_{n,\sigma} (-1)^n \rho_{n,\sigma} + U \sum_{n,\sigma} \rho_{n,\uparrow} \rho_{n,\downarrow}. \quad (1)$$

Here we have used standard notation, namely $c_{n,\sigma}^\dagger$ ($c_{n,\sigma}$) for fermion creation (annihilation) operators and $\rho_{n,\sigma} = c_{n,\sigma}^\dagger c_{n,\sigma}$ for the particle density at site n with spin projection σ . The mass imbalance between fermions is included in the spin-dependent nearest-neighbor ($t_\sigma > 0$) and next-nearest-neighbor ($t'_\sigma > 0$) hopping amplitude respectively, $\Delta > 0$ is the amplitude of the staggered ionic potential and U is the Hubbard interaction strength. Below we assume that the frustration ratio $\zeta = t'_\sigma / t_\sigma$ is spin independent and the mass-imbalance parameter is $\eta = t'_\uparrow / t'_\downarrow = t_\uparrow / t_\downarrow$. Below we restrict our consideration to the case of half-filled band and zero net magnetization $\langle N_\uparrow \rangle = \langle N_\downarrow \rangle = N/2$.

At $\eta = 1$ the model (1) reduces to the Hamiltonian of the $t-t'$ IHM, in the case of half-filled band the prototype model to study the insulator-metal transitions with increasing t' in 1D (see [14] and references therein). At $t'_\sigma = \Delta = 0$ the Hamiltonian (1) reduces to the Hamiltonian of the spin-asymmetric Hubbard model [16], which was introduced to interpolate between the standard Hubbard model ($t_\uparrow = t_\downarrow$) and the Falicov-Kimball model ($t_\uparrow = t$, $t_\downarrow = 0$) [17], and has been intensively studied during the decades. Away from half-filling, the spin-up and spin-down particles are segregated in the ground state of the spin-asymmetric Hubbard model for large enough repulsion [11], while at half-filling the system is an insulator with long-range antiferromagnetic order [12].

The Mean-Field Hamiltonian

Since the translational symmetry of the system is explicitly broken by the Δ term, it is convenient to introduce a unit cell with two sites and operators

$$c_{2m-1,\sigma} = a_{m,\sigma}, \quad c_{2m,\sigma} = b_{m,\sigma}, \quad m = 1, 2, \dots, N/2 \quad (2)$$

and define the mean-field state as GS of the following single-particle Hamiltonian

$$H = \sum_{m,\sigma} \left\{ \left[-t_\sigma a_{m,\sigma}^\dagger (b_{m,\sigma} + b_{m-1,\sigma}) + t'_\sigma (a_{m,\sigma}^\dagger a_{m+1,\sigma} + b_{m,\sigma}^\dagger b_{m+1,\sigma}) + \text{H.c.} \right] - \frac{\Delta_\sigma}{2} (\rho_{m,\sigma}^a - \rho_{m,\sigma}^b) \right\}, \quad (3)$$

where $\rho_{m,\sigma}^a = a_{m,\sigma}^\dagger a_{m,\sigma}$ and $\rho_{m,\sigma}^b = b_{m,\sigma}^\dagger b_{m,\sigma}$ are spin σ fermion density operators on odd (“a”) and even index (“b”) sites respectively and Δ_\uparrow and Δ_\downarrow are variational parameters which minimize the GS energy for the fixed particle filling.

The Hamiltonian (3) can be easily diagonalized in the momentum space. Taking the Fourier transform

$$a_{m,\sigma} = \frac{1}{\sqrt{N}} \sum_k a_{k\sigma} e^{ik(m-1/2)}, \quad b_{m,\sigma} = \frac{1}{\sqrt{N}} \sum_k b_{k\sigma} e^{ikm}. \quad (4)$$

We rewrite the Hamiltonian in the following form

$$H = \sum_{k,\alpha} \left[-2t_\sigma \cos \frac{k}{2} (a_{k\sigma}^\dagger b_{k\sigma} + b_{k\sigma}^\dagger a_{k\sigma}) + 2t'_\sigma \cos k (a_{k\sigma}^\dagger a_{k\sigma} + b_{k\sigma}^\dagger b_{k\sigma}) + \frac{\Delta_\sigma}{2} (a_{k\sigma}^\dagger a_{k\sigma} - b_{k\sigma}^\dagger b_{k\sigma}) \right]. \quad (5)$$

Employing the Bogoliubov rotation

$$a_{k\sigma} = \cos \varphi_{k\sigma} \alpha_{k\sigma} + \sin \varphi_{k\sigma} \beta_{k\sigma}, \quad b_{k\sigma} = -\sin \varphi_{k\sigma} \alpha_{k\sigma} + \cos \varphi_{k\sigma} \beta_{k\sigma},$$

and choosing $\tan 2\varphi_{k\sigma} = 4t'_\sigma \cos(k/2) / \Delta_\sigma$, we obtain

$$H = \sum_{k,\sigma} \left[E_\sigma^+(k) \alpha_{k\sigma}^\dagger \alpha_{k\sigma} + E_\sigma^-(k) \beta_{k\sigma}^\dagger \beta_{k\sigma} \right], \quad (6)$$

where

$$E_\sigma^\pm(k) = 2t'_\sigma \cos k \pm \sqrt{4t_\sigma^2 \cos^2(k/2) + \Delta_\sigma^2 / 4}, \quad (7)$$

and $-\pi \leq k < \pi$.

In GS of the half-filled system, $N/2$ lowest energy states are filled and the rest $N/2$ are empty. For $t'_\sigma = 0$, $E_\sigma^+(k)$ and $E_\sigma^-(k)$ do not overlap and are separated with a direct gap equal to Δ_σ ; all “ α ” – states are occupied whereas all “ β ” – states are empty; the system is in the insulating state. However at $t'_\sigma > t_\sigma^c = 0.5t_\sigma \sqrt{1 + (\Delta_\sigma / 4t_\sigma)^2} + |\Delta_\sigma| / 8$ bands overlap, all the states with energy below the Fermi energy $E_F^\sigma = -t_\sigma^2 / 2t'_\sigma$ are occupied, the system becomes metal with gapless excitation spectrum. One can reverse the problem and determine the value of critical ionicity parameter

$$\Delta_\sigma^c = \begin{cases} 0, & t'_\sigma \leq 0, 5t_\sigma \\ 4t'_\sigma - t_\sigma^2 / t'_\sigma, & t'_\sigma > 0, 5t_\sigma \end{cases} \quad (8)$$

corresponding to the metal-insulator transition point for the given t_σ and t'_σ parameters, respectively. For $|\Delta_\sigma| > \Delta_\sigma^c$ the system is in the insulating phase, while for $|\Delta_\sigma| \leq \Delta_\sigma^c$ in the gapless metallic phase. The energy per site in half-filled GS:

$$E_0^\sigma = \frac{2}{\pi} \left(\frac{t_\sigma}{\kappa_\sigma} \varepsilon(k_{F\sigma}, \kappa_\sigma) - t'_\sigma \sin k_{F\sigma} \right), \quad (9)$$

where $\varepsilon(k_{F\sigma}, \kappa_\sigma)$ is difference between two incomplete elliptic integrals of the second kind:

$$E(k_{F\sigma}, \kappa_\sigma) = E\left(\frac{\pi - k_{F\sigma}}{2}, \kappa_\sigma\right) - E\left(\frac{k_{F\sigma}}{2}, \kappa_\sigma\right), \quad (10)$$

with the modulus $\kappa_\sigma = 1 / \sqrt{1 + (\Delta_\sigma / 4t_\sigma)^2}$ ($0 \leq \kappa_\sigma \leq 1$) and $k_{F\sigma} = 0$ for $|\Delta_\sigma| > \Delta_\sigma^c$ and $k_{F\sigma} = \arcsin\left(\sqrt{(\Delta_\sigma^c)^2 - \Delta_\sigma^2} / 4t'_\sigma\right)$ for $|\Delta_\sigma| < \Delta_\sigma^c$.

Self-Consistency Equations

We close this subsection by evaluating the GS charge distribution and the energy density. The on-site charge density is defined as:

$$\langle \rho_\sigma(n) \rangle = \frac{1}{2} + (-1)^n \delta\rho_\sigma, \quad (11)$$

where $\delta\rho_\sigma$ is a charge imbalance between odd and even sublattices, induced by the ionic Δ_σ term. In half-filled GS $\langle \alpha_{k\sigma}^\dagger \alpha_{k\sigma} \rangle = 1$ for $|k| \geq k_{F\sigma}$ and $\langle \beta_{k\sigma}^\dagger \beta_{k\sigma} \rangle = 1$ for $|k| \geq \pi - k_{F\sigma}$. This gives $\delta\rho_\sigma = \Delta_\sigma \kappa_\sigma \mathcal{F}(k_{F\sigma}, \kappa_\sigma) / 4\pi t_\sigma$, where $\mathcal{F}(k_{F\sigma}, \kappa_\sigma)$ is difference between two incomplete elliptic integrals of the first kind $\mathcal{F}(k_{F\sigma}, \kappa_\sigma) = F\left(\frac{\pi - k_{F\sigma}}{2}, \kappa_\sigma\right) - F\left(\frac{k_{F\sigma}}{2}, \kappa_\sigma\right)$.

Respectively, more common order parameters, characterizing the charge (CDW) and the spin (SDW) density distributions in GS are:

$$\delta\rho_c = \sum_\sigma \delta\rho_\sigma = \sum_\sigma \frac{\Delta_\sigma \kappa_\sigma \mathcal{F}(k_{F\sigma}, \kappa_\sigma)}{4\pi t_\sigma}, \quad \delta\rho_s = -\sum_\sigma \sigma \delta\rho_\sigma = -\sum_\sigma \sigma \frac{\Delta_\sigma \kappa_\sigma \mathcal{F}(k_{F\sigma}, \kappa_\sigma)}{4\pi t_\sigma}.$$

The energy expectation value (per site) of the Hamiltonian (1) with respect to GS of (3) is

$$E_{mf}(\Delta_\uparrow, \Delta_\downarrow) = \sum_\sigma \left[\frac{\Delta_\sigma - \Delta}{2} \delta\rho_\sigma + E_0^\sigma \right] + U \left[\frac{1}{2} + \delta\rho_\uparrow \delta\rho_\downarrow \right]. \quad (12)$$

The variational parameters Δ_\uparrow and Δ_\downarrow are determined from the GS energy minimization requirements. From the extrema of the mean-field GS energy, we obtain the self-consistency (SC) equations:

$$\Delta_\sigma = \Delta - 2U \delta\rho_{-\sigma}. \quad (13)$$

We numerically solved the SC equations (13) to determine the various phases and phase transitions of the model. In the case where solution is not unique, we compare the energies to find out which solution corresponds to the minimum. We fix $t_\uparrow = 1$ and consider the case where all four hopping parameters in units of t_\uparrow are $t_\downarrow = \eta t_\uparrow$, $t'_\uparrow = \zeta t_\uparrow$, $t'_\downarrow = \eta \zeta t_\uparrow$. Under these conditions, the critical staggered potentials are related as $\Delta_\downarrow^c = \eta \Delta_\uparrow^c$. Solutions of the SC equations which corresponds to the minimum of GS energy cluster in following three groups: for both spin projections $|\Delta_\sigma| > \Delta_\sigma^c$ – *insulating* phase and $|\Delta_\sigma| < \Delta_\sigma^c$ – *metallic* state; and yet the third where only one $|\Delta_\sigma|$ is below the critical value and the system is in *half-metallic* state (see Fig. 1). Due to the explicitly broken translational symmetry, for arbitrary $0 < \eta < 1$ all phases are characterized by the coexisting patterns of the alternating charge and spin density modulations (see Fig. 2). At weak repulsion the GS is realized with $\Delta_\downarrow > \Delta_\uparrow > 0$ while at large U with $\Delta_\downarrow > -\Delta_\uparrow > 0$. Thus with increasing U the system experiences transition from a band-insulating phase with dominating CDW order into the correlated-insulating phase with dominating SDW order.

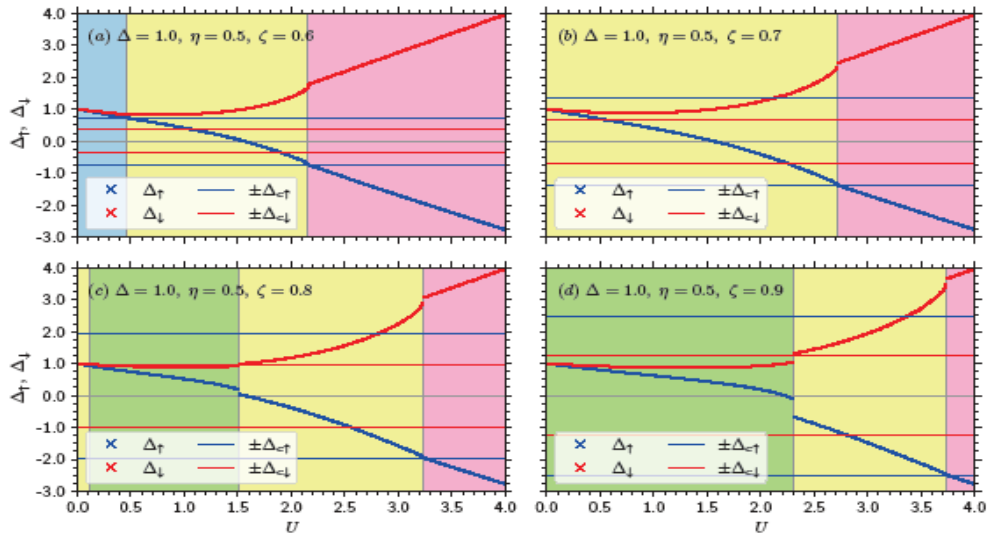


Fig. 1. The variational parameters Δ_{\uparrow} (blue) and Δ_{\downarrow} (red) as a functions of the Hubbard repulsion U for $\Delta=1, \eta=0.5$ and various values of the asymmetry parameter ($\zeta=0.6, 0.7, 0.8, 0.9$). Phase transition points are indicated by vertical dashed lines. Horizontal blue and red lines correspond to critical values of the parameter Δ_{\uparrow}^c (blue) and Δ_{\downarrow}^c (red). The ground state phases are colored in the following way: band-insulator (blue), correlated (Mott) insulator (violet), metal (green) and half-metal (yellow).

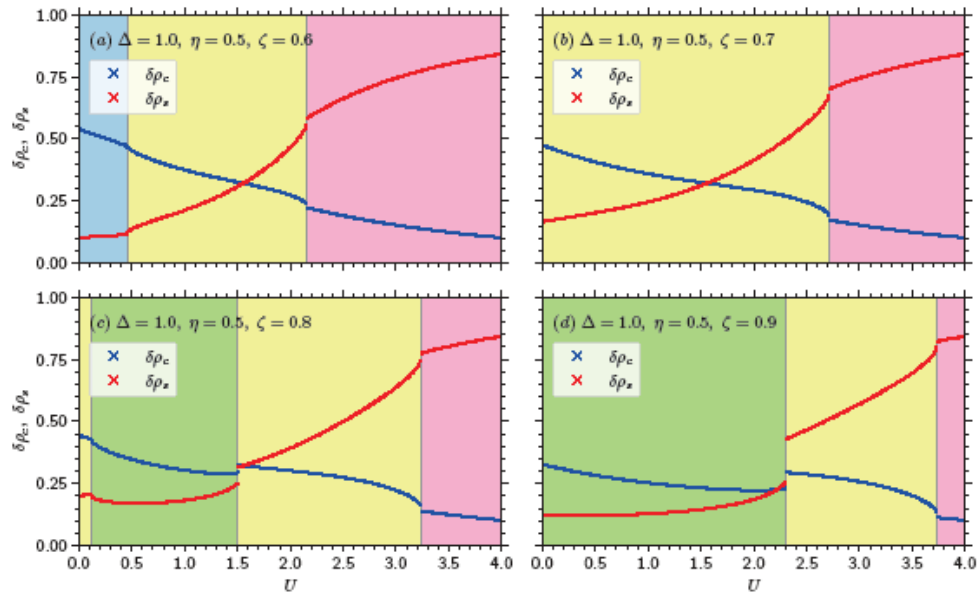


Fig. 2. The charge and spin order parameters as functions of the Hubbard repulsion U for $\Delta=1, \eta=0.5$ and various values of the asymmetry parameter ($\zeta=0.6, 0.7, 0.8, 0.9$). Phase transition points are indicated by vertical dashed lines. The ground state phases are colored in the following way: band-insulator (blue), correlated (Mott) insulator (violet), metal (green) and half-metal (yellow).

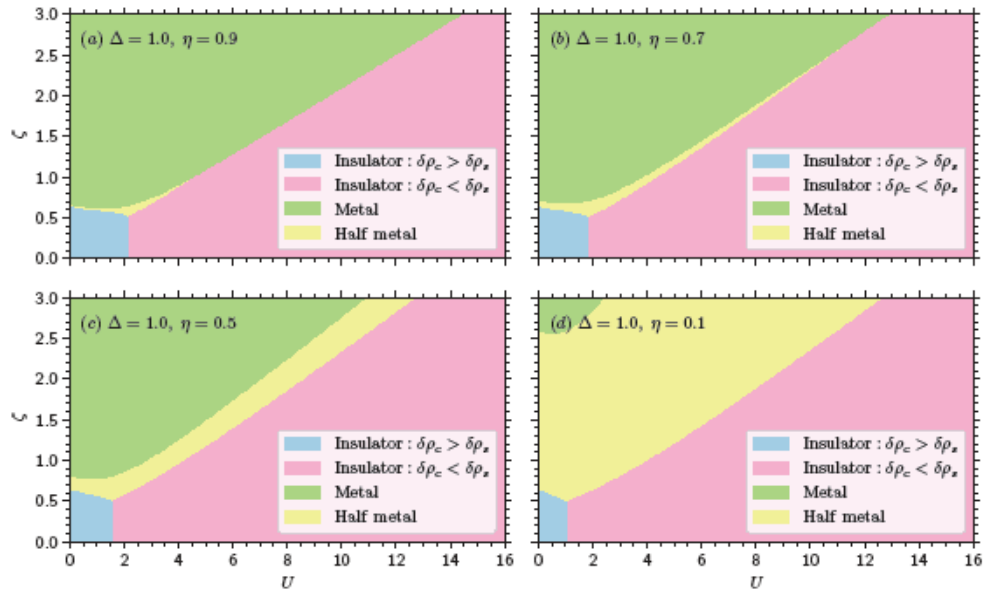


Fig. 3. The ground state phase diagram of the model (1) as a function of the Hubbard repulsion U and frustration parameter ζ for $\Delta = 1$ and various values of the asymmetry parameter ($\zeta = 0.9, 0.7, 0.5, 0.1$). The phases are colored in the following way: band-insulator (blue), correlated (Mott) insulator (violet), metal (green) and half-metal (yellow).

Phase Diagram

Our findings are summarized in Fig. 3. Due to the explicitly broken translation symmetry by the Δ term and mass imbalance, all GS phases are characterized by coexisting long-range-ordered CDW and SDW patterns. At $\zeta < 0.5$ only the insulating phases are realized: with increasing Hubbard repulsion the transition from the BI phase with dominating CDW order at $U < U_c$ into the correlated insulator phase $U > U_c$ takes place. The critical value of the Hubbard repulsion depends on mass-imbalance parameter η and decreases with enhancement of the latter. At $\zeta > 0.5$ the phase diagram is richer. With increasing ζ , both insulating phases are unstable towards transition into the half-metal phase, and with further increase of the frustration ratio, the half-metal phase experience transition in the metal phase. All transitions are of the first order.

The support from the Georgian NSF Grant #FR-19-11872 is gratefully acknowledged.

ფიზიკა

ნახევრად შევსებული $t - t'$ იონური ჰაბარდის ჯაჭვის ძირითადი მდგომარეობის ფაზური დიაგრამა მასათა იმბალანსის პირობებში

შ. გარუჩავა* და გ. ჯაფარიძე**

*ილიას სახელმწიფო უნივერსიტეტი, საბუნებისმეტყველო მეცნიერებათა და მედიცინის ფაკულტეტი, თბილისი, საქართველო

**აკადემიის წევრი, ანდრონიკაშვილის ფიზიკის ინსტიტუტი, თბილისი, საქართველო

საშუალო ველის მიახლოებაში აგებულია ერთგანზომილებიანი ნახევრად შევსებული $t - t'$ იონური ჰაბარდის მოდელის ძირითადი მდგომარეობის ფაზური დიაგრამა სპინზე დამოკიდებული გადახტომებით უახლოეს მეზობლებსა ($t_{\uparrow} \neq t_{\downarrow}$) და ერთის შემდეგ მეზობლებს შორის ($t'_{\uparrow} \neq t'_{\downarrow}$). ფაზური დიაგრამა აგებულია როგორც კინემატიკური ფრუსტრაციის ფარდობის $\zeta = t'_{\sigma} / t_{\sigma}$ და კვანძზე ჰაბარდის განზიდვის U ფუნქცია მასური იმბალანსის პარამეტრის $\eta = t'_{\uparrow} / t'_{\downarrow} = t_{\uparrow} / t_{\downarrow}$ ($0 < \eta < 1$) რამდენიმე მნიშვნელობისათვის ($\zeta = 0.9, 0.7, 0.5, 0.1$). საშუალო ველის მიახლოებაში სისტემა ხასიათდება მოწესრიგების ორი პარამეტრით, Δ_{\uparrow} და Δ_{\downarrow} , რომელთა მნიშვნელობები დგინდება თვითშეთანხმების განტოლებათა სისტემის ამოხსნის შედეგად. რამდენიმე ამონახსნის არსებობის შემთხვევაში გამოიყოფა ის, რომელიც უზრუნველყოფს ძირითადი მდგომარეობის ენერჯის მინიმუმს. ნაჩვენებია, რომ როცა $\zeta < 0.5$ სისტემის ძირითად მდგომარეობაში ხორციელდება მხოლოდ იზოლატორული ფაზები, ზონური იზოლატორის ფაზა როცა $U < U_c$ და კორელირებული იზოლატორის ფაზა როცა $U > U_c$. ფრუსტრაციის ფარდობის გაზრდისას იზოლატორული ფაზები არამდგრადია ჯერ ნახევრად-მეტალურ ფაზაში, ხოლო ζ -ის შემდგომი გაზრდისას – მეტალურ ფაზაში გადასვლის მიმართ. ფაზებს შორის გადასვლები, განპირობებული როგორც ჰაბარდის განზიდვის გაზრდით, ასევე კინემატიკური ფრუსტრაციის ფარდობის ცვლილებით – მიეკუთვნება პირველი გვარის ფაზურ გადასვლათა კლასს.

REFERENCES

1. Wolf S.A., Awschalom D., Buhrman R.A., Daughton J.M., von Molnár S., Roukes M.L., Chtchelkanova A.Y., Treger D.M. (2001) Spintronics: a spin-based electronics vision for the future, *Science* **294**, 5546: 1488–1495.
2. Fang C.M., de Wijs, G.A. and de Groot, R.A. (2002) Spin-polarization in half-metals, *J. Appl. Phys.* **91**, 10: 8340–8344.
3. Lewenstein M., Sanpera A., Ahufinger V. (2012) Ultracold atoms in optical lattices: simulating quantum many-body systems, Oxford University Press, Oxford, UK.
4. Chin C., Grimm R., Julienne P. and Tiesinga E. (2010) Feshbach resonances in ultracold gases, *Rev. Mod. Phys.* **82**, 2: 1225-1285.
5. Messer M., Desbuquois R., Thomas Uehlinger T., Gregor Jotzu G., Sebastian Huber S., Daniel Greif D. and Tilman Esslinger T. (2015) Exploring competing density order in the ionic Hubbard model with ultracold fermions, *Phys. Rev. Lett.* **115**, 11: 115303.
6. Taglieber M., Voigt A.-C., Aoki T., Hänsch T.W., Dieckmann K. (2008) Quantum degenerate two-species Fermi-Fermi mixture coexisting with a Bose-Einstein condensate, *Phys. Rev. Lett.* **100**, 1: 010401.
7. Feiguin A.E., and Fisher M.P.A. (2011) Exotic paired phases in ladders with spin-dependent hopping, *Phys. Rev. B* **83**, 11: 115104.
8. Winograd E.A., Chitra R., Rozenberg M.J. (2011) Orbital-selective crossover and Mott transitions in an asymmetric Hubbard model of cold atoms in optical lattices, *Phys. Rev. B* **84**, 23: 233102.
9. Farkašovský P. (2012) Ferromagnetism in the asymmetric Hubbard model, *Eur. Phys. J. B* **85**, 8: 253.
10. Fáth G., Domański Z., Lemański R. (1995) Asymmetric Hubbard chain at half-filling, *Phys. Rev. B* **52**, 19: 13910-13915.
11. Freericks J.K., Lieb E.H., D. Ueltschi D. (2002) Phase separation due to quantum mechanical correlations, *Phys. Rev. Lett.*, **88**, 106401.
12. Liu W.V., Wilczek F., Zoller P. (2004) Spin-dependent Hubbard model and a quantum phase transition in cold atoms, *Phys. Rev. A*, **70**, 3: 033603.
13. Cazalilla M.A., Ho A.F., Giamarchi T. (2005) Two-component Fermi gas on internal-state-dependent optical lattices, *Phys. Rev. Lett.*, **95**, 226402.
14. Sekania M., Baeriswyl D., Jibuti L., Japaridze G. I. (2017) Mass-imbalanced ionic Hubbard chain, *Phys. Rev. B* **96**, 3: 035116.
15. Bag S., Garg A., Krishnamurthy H. R. (2021) Correlation driven metallic and half-metallic phases in a band insulator, *Phys. Rev. B* **103**, 15: 155132.
16. Brandt U. (1991) Phase separation in the spinless Falicov-Kimball model, *J. Low Temp. Phys.* **84**, 5/6: 477-486.
17. Falicov L.M. and Kimball J.C. (1969) Simple model for semiconductor-metal transitions: Smb6 and transition-metal oxides, *Phys. Rev. Lett.* **22**, 19: 997-1000.

Received January, 2023